Development of Specialized Laser Doppler Velocimeters for High Resolution Flow Profile and Turbulence Spectral Measurements

Donald Ray Brooks

Thesis submitted to the faculty of the Virginia Polytechnic Institute and State University in partial fulfillment of the requirements for the degree of

Master of Science
In
Aerospace Engineering

Kevin T. Lowe
Wing F. Ng
Roger L. Simpson

April 15th, 2014
Blacksburg, Virginia, USA

Keywords: flow measurement techniques, non-intrusive flow measurement, laser flow diagnostics, laser-Doppler velocimetry, laser-Doppler anemometry, turbulence, spectral measurements, spatially resolving, boundary layers, supersonic jets, heated jets

Development of Specialized Laser Doppler Velocimeters for High Resolution Flow Profile and Turbulence Spectral Measurements

Donald Ray Brooks

Abstract

Fluid dynamicists are always in need of innovative instruments for flow velocity measurements. An ideal instrument would be non-intrusive, have a very fine spatial resolution as well as a very fine temporal resolution, be able to measure three-components of velocity, and be compact. Through recent advancements, laser Doppler velocimetry can now meet all of those requirements making it an important part of aerodynamicist's research toolbox.

The first paper presented in this manuscript style thesis explains the development of an advanced three-velocity component, spatially-resolving laser-Doppler velocimetry (LDV) system for highly resolved velocity measurements in situations with limited optical access. The new instrument, a next generation version of the previously developed 'comprehensive' LDV technology, enables measurements of three components of velocity and particle position in the axial direction all through a single transceiving lens. Described here is the design process and the final design for the 'compact, comprehensive' LDV (Comp^{2}LDV). The probe was designed to achieve $\pm 10\ \mu m$ root-mean-square uncertainties in axial particle position, which combined with the long measurement volume, allow researchers to obtain a three-velocity-component velocity statistics profiles over a span of approximately 1.5mm without the need for traversing. Results from measurements in a flat plate turbulent boundary layer very near the wall have compared favorably to data from previous studies.

The second paper focuses on the motion and evolution of coherent structures in supersonic jet flows and how that relates to the intense noise the flows generate. As a preliminary study to experimentally address these relationships, novel non-intrusive measurements using two-component laser Doppler velocimetry (LDV) have been conducted at exceptionally high data rates to lend insight into the statistical behavior of noise-generating flow structures. A new heated supersonic jet facility has been constructed to provide supersonic flow at total temperatures ratios (T_0/T_a) up to 3. In the present work, the instrumentation is validated via comparison of LDV measurements along the centerline of a screeching cold jet with microphone and high-speed shadowgraph results. Reynolds stress spectra are presented for an over-expanded case (nozzle pressure ratio of 3.2) of a design Mach number 1.65 nozzle operated cold (T_0/T_a = 1). A preliminary study was then conducted in the near-nozzle shear layer, up to x/d = 4.0, at design nozzle pressure ratio (4.58) and total temperature ratio of 2.0. Results are presented for Reynolds stress time-delay correlations and power spectra at Re_d = 1.1M for this case. The stream-wise Reynolds normal stress spectra are compared with published spectral behavior reported by other researchers, indicating a similar spectral shape in the downstream stations as previously measured with LDV and hot wire anemometry for cold jets, but which differ in shape from density-based techniques.

Acknowledgements

The path to getting my master's degree has been a wild adventure. I have been fortunate enough to travel to other universities, research centers, and even foreign countries. I am proud that many of the things I have created for this thesis will be used for years to come to advance the Aerospace and Ocean Engineering Department and Virginia Tech. Though it is only briefly mentioned in this report, my crowning achievement is the development and construction of Virginia Tech's heated supersonic jet facility, but none of these things would have been possible without the people who supported me.

I would like to thank my family for never letting me give up on my academic endeavors and for giving me the support and love I needed. I am forever grateful for everything they have done to get me where I am today. Their positive mental attitude kept me from living in a van down by the river. I must thank my friends and Naturally Sharp for keeping me in good spirits.

I owe a huge debt of gratitude to Dr. Todd Lowe for seeing in me what even I couldn't see. On paper, I probably didn't look like a perfect candidate for graduate school, but he saw the drive and ambition that others had over-looked. He took a gamble on me and I can't thank him enough for giving me the opportunity to grow as a professional and contribute to the ever-changing field of aerodynamics. I would also like to thank Drs. Roger Simpson, Wing Ng, William Devenport, and Joseph Schetz for their guidance during my time in grad school and for pushing me to be the great aerodynamicist they knew I could be!

I would also like to thank Tobias Ecker and Dan Cadel for all of their help and friendship as I made my way along the path to graduation. I would also like to thank Pietro Maisto, Mike Nelson, A.J. Wickersham, and David Owens for keeping me grounded throughout this stressful, yet exciting, time.

Finally, none of this would have been possible without the funding from the Office of Naval Research (Drs. Brenda Henderson and Joseph Doychak, program managers) and Pratt and Whitney (Drs. Justin Urban and Andrew Consiglio, program managers) and Applied University Research.

Preamble

The following thesis is written in a manuscript format and contains two papers, both with emphasis on laser Doppler velocimetry. The first paper entitled "Development and Application of a Compact Spatially Resolving Vector Laser Velocimeter for Near Surface Flow Measurements" was presented at the 16th International Symposium on Applications of Laser Techniques to Fluid Mechanics in Lisbon, Portugal in July of 2012. The second paper entitled "Experimental Reynolds Stress Spectra in Hot Supersonic Round Jets" was presented at the 52nd Aerospace Sciences Meeting in National Harbor, Maryland in January of 2014. Both articles presented have multiple authors who contributed to the efforts presented. As lead author on these articles, I was responsible for many aspects of the work including: designing and constructing the hot jet facility and the laser Doppler velocimetery systems, experimental setup and facility operation, instrumentation, literature reviews, article construction and writing, presentation of results, and preparation of figures. All photos presented in this thesis were taken by the author.

Laser Doppler velocimetry (LDV) is a flow measurement technique that has withstood the test of time. Since its introduction in the 1960's [1], the capabilities of the technique have advanced as the supporting technology has advanced. The following thesis will discuss two new laser Doppler velocimeters that have been created by the author and applied to two specific flows.

Many advances have been made in LDV technology in the past decade. Perhaps the most notable is the development of the variable fringe spacing concept first described by Czarske[2] and later generalized for three-dimensional measurements by Lowe and Simpson[3]. Instead of using standard parallel fringes, these LDV's use a pair of beams to create fringes with a gradient; this enables users to determine where within the measurement volume a particle passed through.

The paper entitled "Development and Application of a Compact Spatially Resolving Vector Laser Velocimeter for Near Surface Flow Measurements"[4] covers the design and validation of an LDV system for measurement of three components of velocity with a very fine axial spatial resolution. The design employs a variable fringe pattern to accurately resolve the position of measured particles in the measurement volume. A rigorous design study was performed to optimize the uncertainty in the velocity and position measurements. A validation of the system was performed in a turbulent boundary layer facility at Virginia Tech. This paper is currently in the process of being converted to a journal article.

While the LDV technique has matured, so has the supporting technology. New commercially available components have increased the speed at which data can be collected and processed. These new developments have enabled researchers to investigate smaller turbulent time scales than ever before. This is an important capability for supersonic jet flows. Previous work done by Kerhervé et al.[5] in 2004 were able to achieve data rates over 10 kHz, but at Virginia Tech in 2014 we are now able to get data rates over 100kHz.

The paper entitled "Experimental Reynolds Stress Spectra in Hot Supersonic Round Jets"[6]uses a two-component LDV system, similar to the system described in the first paper, to acquire velocity measurements at a high data rate in a cold and heated Mach 1.65 supersonic jet flow. The high data rates allowed the data to be post-processed for turbulence spectra. The cold jet test was performed at an over-expanded screeching condition and the heated tests were performed at the design condition for the nozzle and a total temperature ratio of $T_0/T_a = 2$.

These tests were performed in Virginia Tech's new supersonic hot jet rig. The results of this study validated not only our facility, but also our ability to measure in this violent flow. The Reynolds stress spectra that we measured showed good agreement to the results of Kerhervé et al.[4]. With this knowledge we can now begin more studies in this facility with this LDV. The next planned measurements are to be similar to the heated jet conditions that are presented in this thesis but with a finer test grid. The acquired data will first be processed for acceleration measurements.

[1]Yeh Y, and Cummins HZ, "Localized Fluid Flow Measurements with an HeNe Laser Spectrometer," 1964; App Phys Letts Vol. 4, pp. 176-78.

[2]Czarske J, Büttner L, Razik T, Müller H. "Boundary layer velocity measurements by a laser Doppler profile sensor with micrometre spatial resolution". Measurement Science and Technology. 2002; 13(12):1979-1989.

[3]Lowe KT, Simpson RL. Turbulence structural measurements using a comprehensive laser–Doppler velocimeter in two- and three-dimensional turbulent boundary layers. International Journal of Heat and Fluid Flow. 2008; 29(3):820-829.

[4]Brooks DR, Lowe KT. "Development and application of a compact spatially resolving vector Laser velocimeter for near surface flow," 16th Intl. Symp. on Applications of Laser Techniques to Fluid Mechanics, Lisbon, Portugal, 9-12 July, 2012, Paper #303.

[5]Kerhervé, F., Jordan, P., Gervais, Y., Valière J.C., Braud, P., "Two-Point Laser Doppler Velocimetry Measurements in a Mach 1.2 Cold Supersonic Jet for Statistical Aeroacoustic Source Model," Exp. In Fluids, Vol. 37, 2004, pp. 419-437. 2014:1-10.

[6]Brooks DR, Ecker T, Lowe K, Ng W. Experimental Reynolds Stress Spectra in Hot Supersonic Round Jets. 2014

Table of Contents

List of Figures

List of Tables

1 Paper #1: Development and Application of a Compact Spatially Resolving Vector Laser Velocimeter for Near Surface Flow Measurements

1.1 Abstract

The need for highly resolved velocity measurements in situations with limited optical access has driven the development of an advanced three-velocity component, spatially-resolving laser-Doppler velocimetry (LDV) system. The new instrument, a next generation version of the previously developed 'comprehensive' LDV technology, enables measurements of three components of velocity and particle position in the axial direction all through a single transceiving lens. Described here is the design process and the final design for the 'compact, comprehensive' LDV (Comp^{2}LDV). The probe was designed to achieve $\pm 10\ \mu m$ root-mean-square uncertainties in axial particle position, which combined with the long measurement volume, allow researchers to obtain a three-velocity-component velocity statistics profiles over a span of approximately 1.5mm without the need for traversing. Results from measurements in a flat plate turbulent boundary layer very near the wall have compared favorably to data from previous studies.

1.2 Introduction

Currently, a major drawback of single-head three-velocity component laser-Doppler velocimeter (LDV) probes is the poor axial spatial resolution of the probe volumes. Presented here is an LDV design and proof-of-concept of a single-head velocity vector LDV which mitigates this conventional resolution shortcoming by achieving 10μm root-mean-square axial spatial resolution by the variable fringe spacing concept.

This new instrument brings together the ability to measure vector velocity with fine axial spatial resolution through one transceiving lens. The benefits of such a capability may enable researchers to explore flows with limited optical access such as harsh reacting flows in the corners of high speed flow facilities. The probe also has the ability to measure near surfaces throughout a broad speed range, anywhere from low speed to supersonic flows. As this technology is a compacted version of the 'comprehensive' LDV technology pioneered by Lowe and Simpson[1], it has been given the name, 'compact, comprehensive' laser-Doppler velocimeter (Comp^{2}LDV).

The Comp^{2}LDV employs the variable fringe spacing concept first described by Czarske[2] and later generalized for three-dimensional measurements by Lowe and Simpson[1]. Fringe gradients greatly enhance spatial-resolution by creating a unique variation of the fringe spacing along the bisector of the two interfering beams. The resulting fringe patterns can either be

converging or diverging, depending up on the position of the beam waist relative to the measurement volume[3]. In the case of the Comp[2]LDV, a converging fringe pattern was chosen, meaning that the fringe spacing becomes smaller with distance from the probe in the measurement volume (Figure 1.1). The pair of beams creating the converging fringe pattern is accompanied by measurement volumes created similar to classical LDV systems, with beam crossed at their waists. By comparing the signal from the converging fringe pattern to the velocity measured by the conventional LDV volumes, the local fringe spacing of the converging fringe volume may be deduced, yielding a measure for position (as in Figure 1.1 at the right).

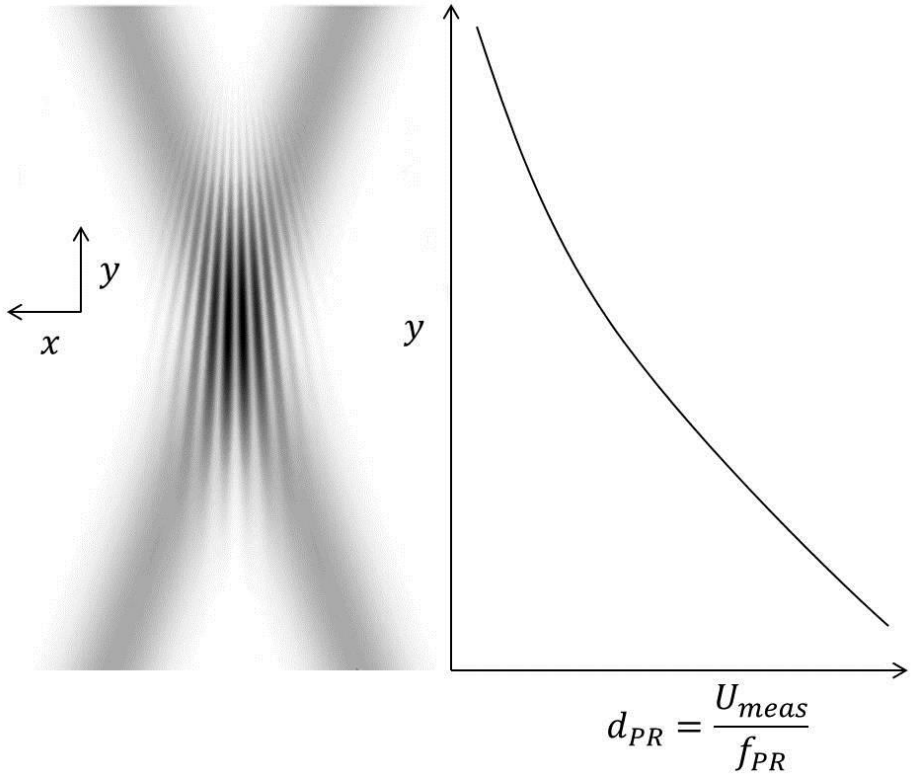

Figure 1.1: Diagram of a converging fringe pattern (left). The particle crossing position along direction y may be inferred by employing the dual-beam LDV equation using the measured velocity and the Doppler frequency to obtain the local converging fringe spacing, d_{PR}.

With the ability to measure vector velocities at high special resolution through one transceiving lens, this instrument is well-suited for studies in high Reynolds number turbulent boundary layers. Future work will leverage the technique in square exit supersonic jet nozzles for detailed nozzle internal boundary layer and corner flow characterization. It will also be used to measure shear layers in the near fields of the jets and high gradient regions.

1.3 Previous Work

Limited optical access can be a problem with a wide variety of experimental setups. The simplest single-head LDV configuration is that which only measures one component of velocity[4]. Using a "1D-LDV" becomes impractical when a researcher wishes to measure multiple components of velocity. A 1D-LDV can be rotated to change which component of velocity is being measured, and multiple 1D-LDV probes can be used to simultaneously measure three components; however, such a system is no longer "single-headed", thus making it difficult to use with limited optical access. Naturally, the next step is to increase the number of components to two, creating a "2D-LDV" [5]. Typically, a 2D-LDV can be designed to utilize either four beams or three beams to create the interfering beam pairs. If the design is chosen to utilize three beams then either wavelength, carrier frequency, or polarization discrimination must be used[6,7]. Finally, a single-headed "3D-LDV" can be created to fully characterize flows with limited optical access[8,9], though such a system suffers poor axial spatial resolution and limited axial velocity resolution.

The new Comp^{2}LDV is similar to that created by Stauter[8], in the way that the current probes utilizes five beams to measure three components of velocity using only a single head. The Comp^{2}LDV also contains an additional pair of beams, which are used to give the probe spatial resolution in the axial direction as previously described.

1.4 Instrumentation Design

The design of this probe was driven by the goal of low uncertainties, in both velocity and position, using only one transceiving lens. In order to measure three components of velocity and provide spatial resolution in the axial direction, four interfering beam pairs must be used. Seven beam produce the interfering pairs required: two beams interfere to measure predominantly the axial velocity, three beams interfere to measure the transverse direction, and two beams interfere enable the spatial resolution in the axial direction. It was decided that the probe would utilize a 50.8 *mm* diameter transceiving lens. From this design constraint many beam configurations and transceiving lens focal lengths were analyzed in a parametric trade study to achieve minimum uncertainties for the measured quantities of the probe, particularly the velocity and position in the axial direction. The final parameters chosen from this study are listed in Table 1.1.

Table 1.1: Geometric and beam parameters of the Comp^{2}LDV

Parameter	Value
Transceiving Lens Focal Length	150 *mm*
Transceiving Lens Diameter	50.8 *mm*
Nominal Fringe Spacing	4 μm
Collimating Lens Focal Length	1.45 *mm*
CompLDV Collimating lens Focal Length	30 *mm*
CompLDV Collimating Lens Diameter	8 *mm*
Measurement Volume Diameter	280 μm
Number of Fringes	72
Axial Measurement Volume Length (Based on Beam Geometry)	4.4 *mm*

A standard fiber optic beam delivery system was used to power the probe. The '7-beam' probe configuration in which two beams are coupled into one fiber transmitted along the probe optical axis, as implemented by past researchers[8,10], enabled the minimum axial velocity uncertainty for the dual-beam mode operation. The six beams that are emitted from the probe intersect to form the measurement volume. The chosen beam configuration can be seen in the front view of the probe presented in Figure 1.2; the polarization direction of the beams are depicted by lines drawn in each laser collimating lens, with lines of the same color representing sets of interfering beams. The components of velocity that are directly measured are represented in a Cartesian coordinate system, with *z* along the optical axis, as follows:

$$\begin{aligned} \hat{b}_{1-2} &= 0.7056\hat{\imath} \;\; - 0.7056\,\hat{\jmath} \; + \; 0.0656\hat{k} \\ \hat{b}_{3-2} &= -0.7056\hat{\imath} \;\; - 0.7056\hat{\jmath} + \;\; 0.0656\hat{k} \\ \hat{b}_{4-5} &= \; -0.9978\,\hat{\imath} - 0.0664\hat{k} \end{aligned} \tag{1.1}$$

Where the subscript on $\hat{b}$ denotes the numbers of the beams used for that fringe-forming pair. A simple set of linear equations can be used to extract three orthogonal components of velocity from the components measured along the directions in Equations (1.1).

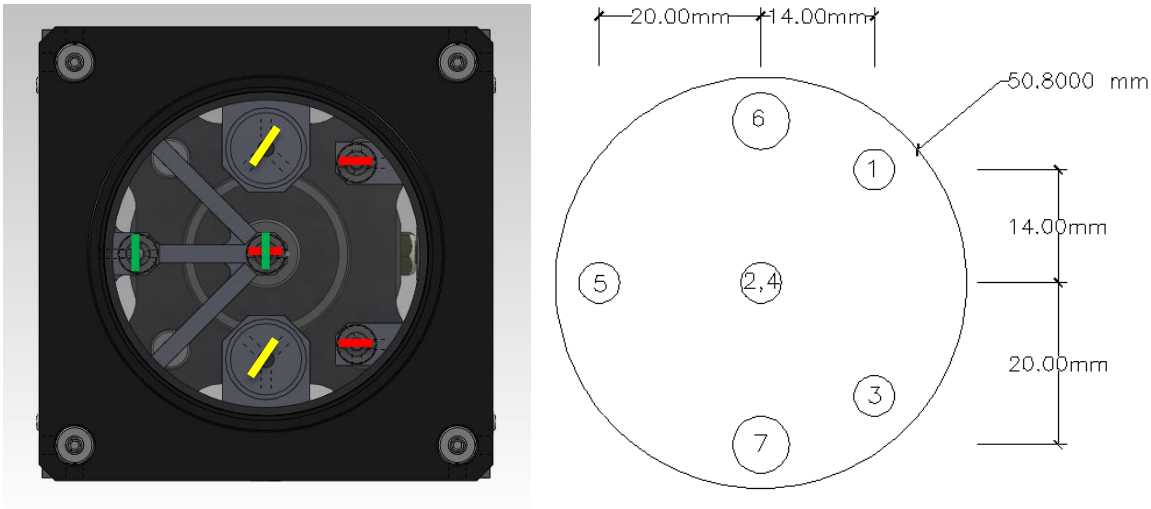

Figure 1.2: Front view of the compact, comprehensive LDV. The directions of the lines in the front view indicate the polarization axes of the beams; lines of like color interfere to form fringes.

The transceiving lens of diameter 50.8 *mm* was chosen to be an achromat lens to minimize spherical and chromatic aberrations. The lens is mounted to the probe using a Thorlabs adjustable lens mount. The lens mount was in turn mounted to a 60 *mm* "cage system" from Thorlabs. At the rear of the probe an x-y translating ST fiber plate was mounted to a 30 *mm* cage system. Custom fiber optics and collimating lens mounts of 303 stainless steel, with reduced coefficient of linear expansion compared to aluminum, were developed for the probe and featured 0-80 set screws for alignment of the individual beams. A rendering of the assembled probe can be seen in Figure 1.3.

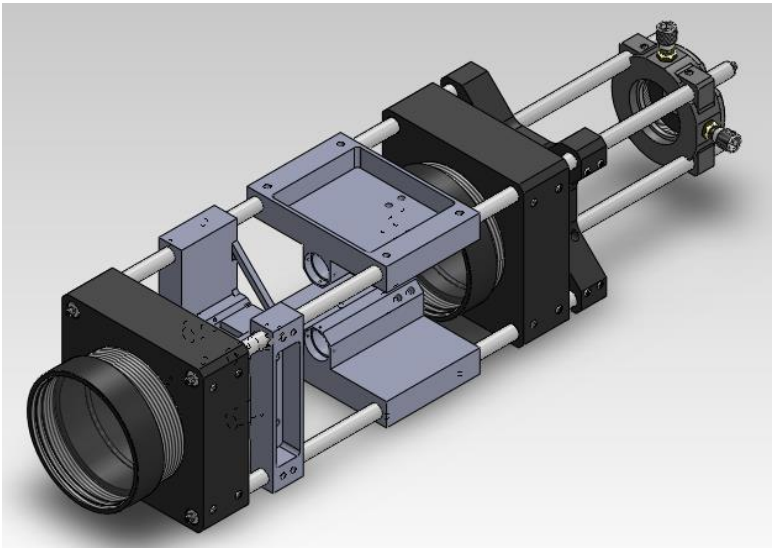

Figure 1.3: Isometric rendering of the Comp^{2}LDV.

Two Coherent Innova Argon-ion gas lasers in single line mode at 514.5 *nm* are used to produce the five beams for the three components of velocity and a Coherent Verdi-6W diode-pumped solid state ($Nd:YVO_4$) laser doubled to emit at 532 *nm* is used to power the beams for the converging fringe volume, providing the axial spatial-resolution.

1.5 Uncertainty Analysis

As with any measurement technique, calculating and controlling uncertainty in the acquired data is of the utmost importance. In this system there are two main uncertainties to account: position and instantaneous velocity. As previously mentioned, a parametric trade study was done to minimize the uncertainties. The only information necessary to begin the trade study were various beam configurations. The vectors of the beams were reduced to find the angle of intersection between the two interfering beams. The following analysis is done for the final chosen beam configuration, but the reader should bear in mind that this analysis was done for multiple configurations.

The uncertainties in the instantaneous velocity can be found by

$$\delta U, \delta V, \delta W = \sqrt{(d\delta f)^2 + (f\delta d)^2} \tag{1.2}$$

where $\delta U, \delta V, \delta W$ are the uncertainties in the three components of velocity, d is the fringe spacing, δd is the uncertainty in the fringe spacing, f is the measured Doppler frequency, and δf is the uncertainty in the measured frequency. Equation (1.2) can be further simplified using the dual beam LDV equation $f_{doppler} = U_{\perp}/d$,

$$\frac{\delta U}{U} = \sqrt{\left(\frac{\delta f}{f}\right)^2 + \left(\frac{\delta d}{d}\right)^2} \tag{1.3}$$

One may approximate the uncertainty in the frequency to be $\delta f/f = 0.1/T$ where T is the duration of the burst signal[11]. The duration of the burst can be related to diameter of the measurement volume and measured instantaneous velocity as $T = \sin\beta\, D/U$, where D is the diameter of the measurement volume which is 280 μm and β is the angle formed between the axial direction of the probe and the direction of the flow which is 90°. Table 1.2 contains all of the resulting values for the uncertainty analysis.

Table 1.2: Results of the uncertainty analysis of the velocity measurements of the Comp^{2}LDV

$D\ (\mu m)$	$d_{1,2,3}\ (\mu m)$	$d_{4,5}\ (\mu m)$	δU (%)	δV (%)	δW (%)
280	3.921	4.0034	0.14	1.25	0.14

The uncertainty in the position measurement requires special treatment as compared to that of the instantaneous velocity. The velocity that is measured by the converging fringes can be represented by,

$$U_{comp} = sin\beta U - cos\beta W \tag{1.4}$$

Again, for the experimental setups of this probe, β will be 90˚ meaning it only measures *U* velocity. From the previous uncertainty analysis for the instantaneous velocity, we know that the uncertainty of the measurement of *U* velocity is 0.14%. The fringe spacing within the measurement volume is known to be the instantaneous velocity divided by the instantaneous Doppler frequency. The uncertainty in the value of the fringe spacing due to uncertainties in the measured Doppler frequency and the instantaneous measured velocity can be found by rearranging Equation (1.3) to obtain,

$$\frac{\delta d}{d} = \sqrt{\left(\frac{\delta f}{f}\right)^2 + \left(\frac{\delta U}{U}\right)^2} \tag{1.5}$$

Using the previous expression that, $\delta f = 0.1/T$, where $T = \sin\beta\, D/U$ and $U = d * f$, it's found that,

$$\frac{\delta f}{f} = \frac{0.1Ud}{sin\beta DU} = \frac{0.1d}{sin\beta D} \tag{1.6}$$

Equation (1.6) can be further simplified with the relation that the number of fringes (N_f) is the fringe spacing divided by the diameter of the measurement volume, which results in,

$$\frac{\delta f}{f} = \frac{0.1}{sin\beta N_f} \tag{1.7}$$

For a converging fringe pattern, the axial variation in the fringe spacing can be described by for Gaussian beams[3],

$$d(y) = \frac{\lambda}{2\sin\varphi}\left(1 + \frac{y\cos^2\varphi\,(y\cos^2\varphi - y_W)}{y_R^2\cos^2\varphi - y_W(y\cos^2\varphi - y_W)}\right) \tag{1.8}$$

where y is the distance in the axial direction in the measurement volume, y_W is the distance between the waist of the beam and the center of the measurement volume, φ is half of the angle of intersection of the beams, λ is the wavelength of the light, and y_R is defined as,

$$y_R = \frac{\pi \omega_0^2}{\lambda} \tag{1.9}$$

where ω_0 is the radius of the beam at the waist. Equation (1.8) can be replaced with a very simple model for the variation of converging fringes as discussed by Lowe[12],

$$d(y) = Ay + d_0 \tag{1.10}$$

Where *A* is the first-order Taylor series expansion for the fringe gradient,

$$A = \frac{d_0 y_w}{[y_R^2 + (y_w/cos\varphi)^2]} \tag{1.11}$$

and d_0 is the fringe spacing at the center of the measurement volume ($y = 0$). When comparing the Gaussian fringe distribution to the simple linear expansion, it is found that the RMS difference between the two, weighted by the number of samples found at each fringe spacing, is 3.16 μm.

It is crucial to determine the uncertainty in the measured fringe spacing, which will directly relate to the uncertainty in the measurement of the axial particle position. This uncertainty relation is,

$$\delta y = \frac{\delta d}{A} \tag{1.12}$$

Substituting Equation (1.11) into Equation (1.12),

$$\delta y = \frac{\delta d}{d} \frac{[y_R^2 + (y_w/cos\varphi)^2]}{y_w} \tag{1.13}$$

The parameters and results of implementing Equations (1.5) and (1.13) for position uncertainty are listed in Table 1.3.

Table 1.3: Results of the uncertainty analysis of the position measurements of the Comp^{2}LDV

$\delta f/f$	$\varphi\ (rad)$	$\lambda\ (nm)$	$\omega_0\ (\mu m)$	$y_w\ (\mu m)$	$y_R\ (\mu m)$	$d(y)_{Gauss}$	A, m/m	$\delta y\ (\mu m)$
7.15e-4	0.266	532	7.0	5800	290	[1.5-3.0]	3.2e-4	7.8

1.6 Concept Validation

Following the completion of the optical and laser setup used to provide the necessary interfering beam sets, concept validation for the Comp^{2}LDV probe began. Presented here are the results from the validation measurements that took place in the small boundary layer tunnel at Virginia Tech (Figure 1.4). This tunnel was designed to produce a constant temperature, constant velocity flow, and the floor turbulent boundary layer has been well characterized[12].

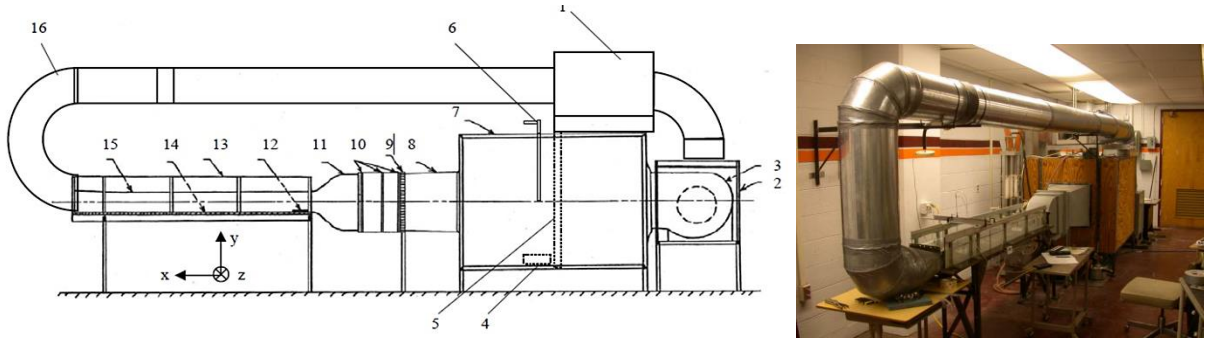

1.Air Conditioner	5. Baffle Plat	9. Honeycomb	13. Glass Side Walls
2. Filter Box	6. Seeding Pipe	10. Screens	14. Bottom Wall
3. Blower	7. Plenum Chamber	11. Contraction	15. Top Wall
4. Drip Pan	8. Contraction	12. Trip Arrangement	16. Return Ducting

Figure 1.4: Diagram of the Department of Aerospace and Ocean Engineering small boundary layer wind tunnel.

The tunnel facility was originally outfitted with a test section floor made of quarter inch thick standard float glass to allow for optical accessibility. Unfortunately, the quality of the window inhibited near wall measurements. The test section floor was changed to an aluminum plate with a single 25.4 *mm* diameter anti-reflection coated window. This new floor panel along with the probe mounted under the tunnel can be seen in Figure 1.5. It was also found that rotating the probe by a 12° angle from vertical reduced the amount of light being reflected back into the probe head, as previously described by Stauter[8].

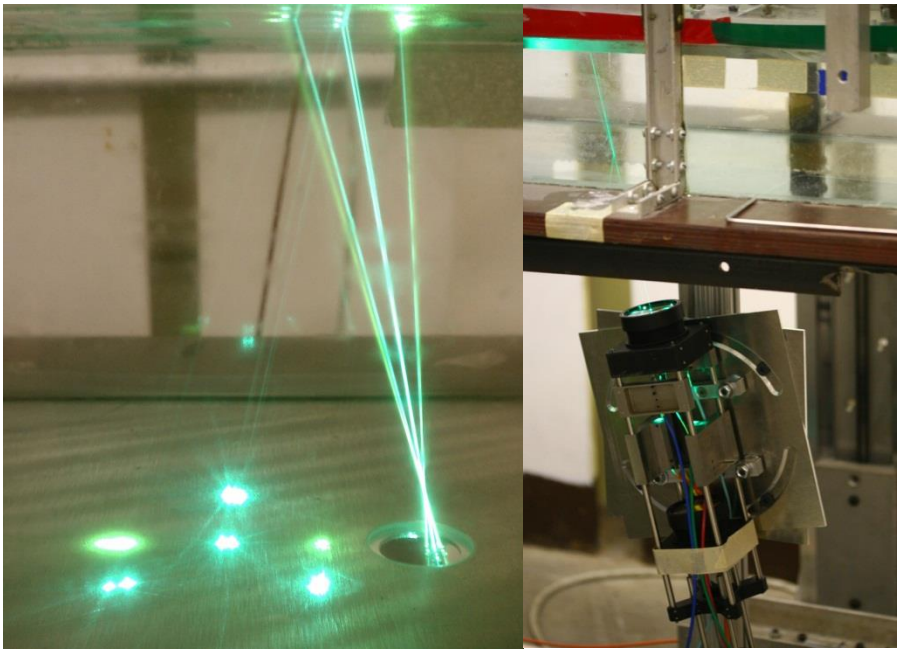

Figure 1.5: Photos of the new floor panel and the compact, comprehensive LDV, mounted under the tunnel.

For this concept validation the law-of-the-wall region of the floor turbulent boundary layer was measured without traversing the probe. Confidence is obtained in the validation by comparing the mean stream-wise velocity data with previous results of DeGraaff and Eaton[13] at $Re_\theta = 5160$ and Lowe and Simpson (2009) at $Re_\theta = 7500$. For comparison the acquired velocities are normalized by the wall shear velocity (u_τ). The acquired data are also compared to the linear viscous sublayer region and the logarithmic law-of-the-wall. In the viscous sublayer[14],

$$U^+ = y^+ \tag{1.14}$$

where $U^+ \equiv U/u_\tau$ and $y^+ \equiv y/\delta_\nu$. The wall friction velocity is defined as $u_\tau = \sqrt{\tau_w/\rho}$, where τ_w is the wall shear stress and ρ is the fluid density. The viscous length scale is defined as $\delta_\nu = \nu/u_\tau$, where ν is the kinematic viscosity. The logarithmic region is defined as

$$U^+ = \frac{1}{\kappa}\ln y^+ + B \tag{1.15}$$

Where κ and B are constants. Coles[15] gives these values to be $\kappa = 0.41$ and $B = 5.0$.

Comparison of the velocity statistics to those of DeGraaff and Eaton[13], Lowe and Simpson[16], and the law-of-the-wall equations is satisfactory (Figure 1.6). The data plotted in gray in Figure 1.6, are the individual burst acquired, whose position-binned averages make up the black line in the figure.

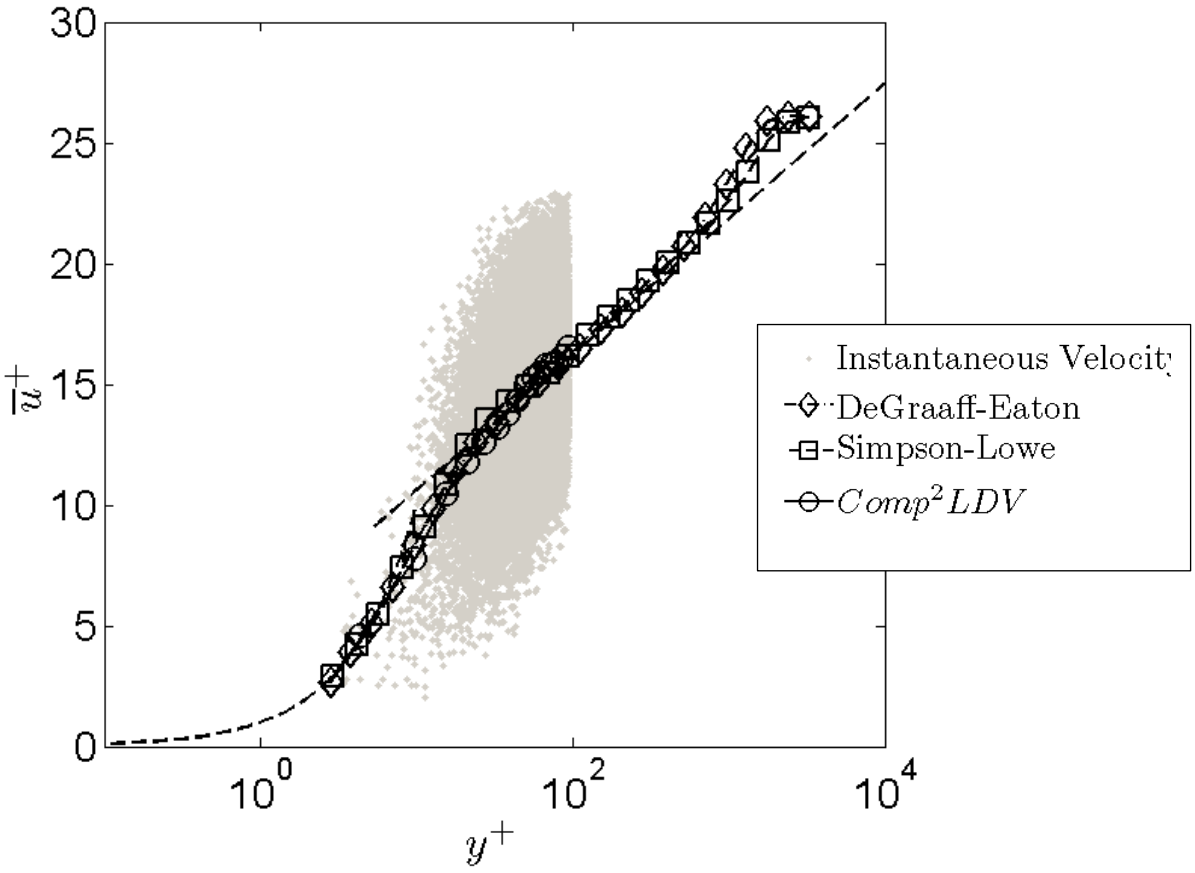

Figure 1.6: Resolved near wall profile for the mean stream-wise velocity in viscous wall scaling. The dashed line in this plot is the viscous sublayer relationship, $\bar{U}^+ = y^+$. Comparison data previous studies from Lowe and Simpson[16] (2009, $Re_\theta = 7500$) and DeGraaff and Eaton[13] (2000, $Re_\theta = 5160$).

In Figure 1.7 (a,b,c), the stream-wise and normal-to-the wall Reynolds normal stress statistics are compared with the results of DeGraaff and Eaton[13] and Lowe and Simpson[16] using wall scaling. Of particular note is the quality of comparison of the normal-to-wall normal stress measurements, as this direction is the one with most uncertainty in for the Comp^{2}LDV configuration. The results indicate that adequate uncertainties for wall-measurements of even the important normal component are possible in this compact arrangement. Measurements of span-wise normal stress and Reynolds shear stress are presented in Figure 1.7d, along with comparator data. Again, the normal-to-wall fluctuation measurement is well-behaved in the Reynolds shear stress, lending further confidence in the concept.

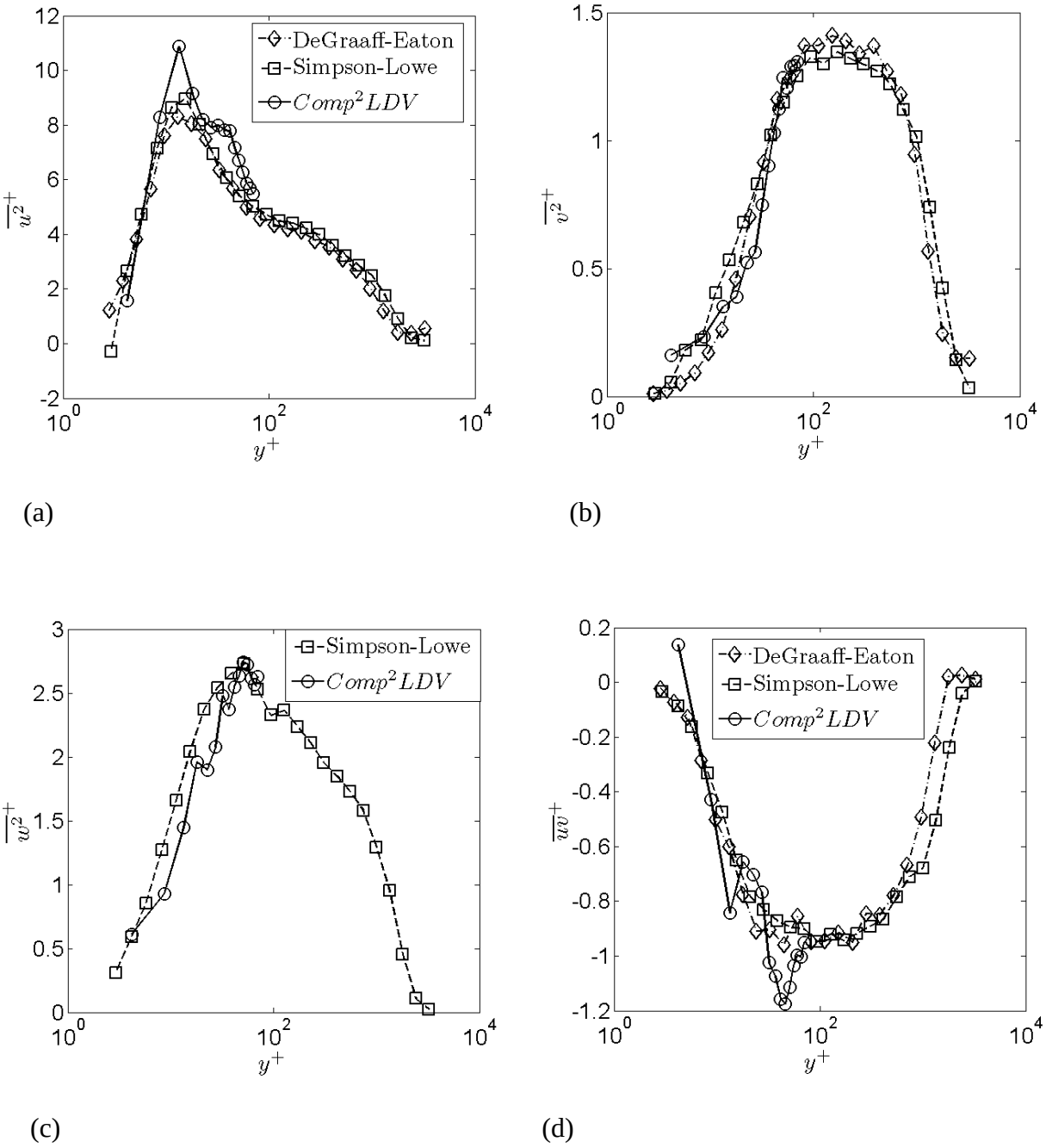

Figure 1.7: Resolved profiles for the Reynolds stresses in viscous wall scaling. (a) stream-wise normal stress; (b) normal-to-wall normal stress; (c) span-wise normal stress; (d) Reynolds shear stress. The data obtained by the Comp^{2}LDV favorably matches the data obtained by previous studies from Lowe and Simpson[16] (2009, $Re_\theta = 7500$) and DeGraaff and Eaton[13] (2000, $Re_\theta = 5160$).

1.7 Future Work

The Comp^{2}LDV will be used extensively for fundamental studies of high Reynolds number flows with very large velocity gradients. Measurements are currently underway to characterize the boundary layer at the exit of a transonic jet (Figure 1.8). The ultimate goal of this probe is to measure square exit supersonic jet nozzles with over expanded flow for detailed nozzle internal boundary layer and corner flow characterization. This is to be done by using a custom made nozzle with three walls made of glass to allow optical access (Figure 1.9).

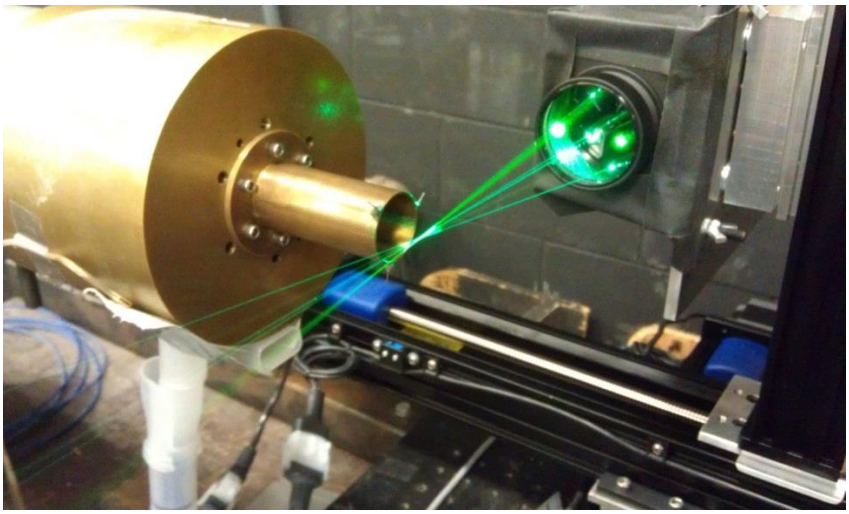

Figure 1.8: Photo of the Comp^{2}LDV mounted to measure the velocity at the exit of the transonic jet.

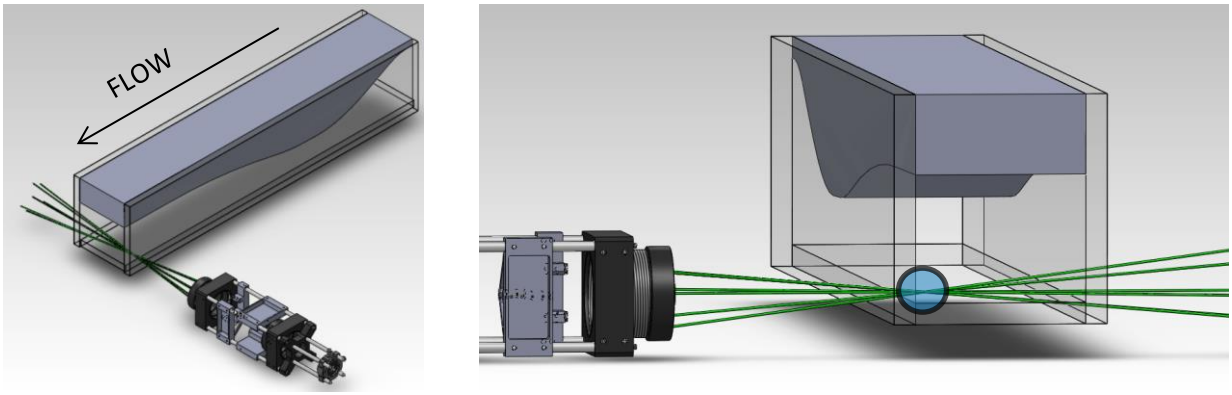

Figure 1.9: Diagram of the Comp^{2}LDV measuring the boundary layer in the square exit nozzle. The area of highly-resolved vector velocities measured can be seen circled in blue within microns of the duct corner.

1.8 Conclusions

The new Comp^{2}LDV instrument, validated in a turbulent boundary layer, gives researchers the ability to measure three dimensions of velocity at high axial spatial resolution using only one probe head. It also combines the velocity measurements with $\pm 8\mu m$ spatial-resolution in the axial direction, thus solving the resolution limitations of past single-head concepts. Due to the instrument only having one transceiving lens, researchers may explore flows with limited optical access such as high speed corner flows.

1.9 Acknowledgments

The authors would like to acknowledge the support of the Virginia Tech Department of Aerospace and Ocean Engineering and the Office of Naval Research (Drs. Brenda Henderson and Joseph Doychak, program managers). We would also like to acknowledge the machinists of the Department of Aerospace and Ocean Engineering for the precision parts produced for the probe. We also acknowledge Applied University Research and Dr. Roger Simpson for the use of AUR Studio, the LDV acquisition software used.

1.10 References

[1]Lowe KT, Simpson RL. Turbulence structural measurements using a comprehensive laser–Doppler velocimeter in two- and three-dimensional turbulent boundary layers. International Journal of Heat and Fluid Flow. 2008;29(3):820-829.

[2]Czarske J, Büttner L, Razik T, Müller H. Boundary layer velocity measurements by a laser Doppler profile sensor with micrometre spatial resolution. Measurement Science and Technology. 2002;13(12):1979-1989.

[3]Miles P. Geometry of the fringe field formed in the intersection of two Gaussian beams. Applied Optics. 1996:1-9.

[4]Ahmed NA, Elder RL, Forster CP, Jones JD. Miniature laser anemometer for 3D measurements. Measurement Science and Technology. 1990;1(3):272-276.

[5]Huffaker R. Laser Doppler detection systems for gas velocity measurement. Applied Optics. 1970:1-14.

[6]Pannell CN, Tatam RP, Jones JD, Jackson DA. Two-dimensional fibre-optic laser velocimetry using polarisation state control. Journal of Physics E: Scientific Instruments. 1988;21(1):103-107.

[7]Czarske JW. Laser Doppler velocimetry using powerful solid-state light sources. Measurement Science and Technology. 2006;17(7):R71-R91.

[8]Stauter RC. Measurement of the Three-Dimensional Tip Region Flow Field in an Axial Compressor. Journal of Turbomachinery. 1993;115(3):468.

[9]Byrne GD, James SW, Tatam RP. A single-headed fibre optic laser Doppler anemometer probe for the measurement of flow angles. Measurement Science and Technology. 2004;15(1):1-8.

[10]Charrett TO, James SW, Tatam RP. Optical fibre laser velocimetry: a review. Measurement Science and Technology. 2012;23(3):032001.

[11]Shinpaugh K, Simpson R, Wicks al, Ha S. Signal-processing techniques for low signal-to-noise ratio laser Doppler velocimetry signals. Experiments in. 1992:1-10.

[12]Lowe KT. Design and application of a novel Laser-Doppler Velocimeter for turbulence structural measurements in turbulent boundary layers. 2006:1-292.

[13]DeGraaff D, Eaton J. Reynolds-number scaling of the flat-plate turbulent boundary layer. Journal of Fluid Mechanics. 2000:1-28.

[14]Rotta J. Turbulent boundary layers in incompressible flow. Progress in Aerospace Sciences. 1962.

[15]Coles D. The law of the wake in the turbulent boundary layer. Journal of Fluid Mechanics. 1956:1-36.

[16]Lowe KT, Simpson RL. An advanced laser-Doppler velocimeter for full-vector particle position and velocity measurements. Measurement Science and Technology. 2009;20(4):045402.

2 Paper #2: Experimental Reynolds Stress Spectra in Hot Supersonic Round Jets

2.1 Abstract

The motion and evolution of coherent structures in supersonic jet flows is directly related to the intense noise the flow generates. As a preliminary study to experimentally address these relationships, novel non-intrusive measurements using two-component laser Doppler velocimetry (LDV) have been conducted at exceptionally high data rates to lend insight into the statistical behavior of noise-generating flow structures. A new heated supersonic jet facility has been constructed to provide supersonic flow at total temperatures ratios ($\mathbf{T_0/T_a}$) up to 3. The new LDV used here allows for highly spatially and temporally resolved measurements of velocity in the hot supersonic jet under study. In the present work, the instrumentation is validated via comparison of LDV measurements along the centerline of a screeching cold jet with microphone and high-speed shadowgraph results. LDV results for the local appearance of screech tones and harmonics in the Reynolds stress spectra are presented for an over-expanded case (nozzle pressure ratio of 3.2) of a design Mach number 1.65 nozzle operated cold ($\mathbf{T_0/T_a}$ = 1). A preliminary study was then conducted in the near-nozzle shear layer, up to x/d = 4.0, at design nozzle pressure ratio (4.58) and total temperature ratio of 2.0. Results are presented for Reynolds stress time-delay correlations and power spectra at Re_d = 1.1M for this case. The stream-wise Reynolds normal stress spectra are compared with published spectral behavior reported by other researchers, indicating a similar spectral shape in the downstream stations as previously measured with LDV and hot wire anemometry for cold jets, but which differ in shape from density-based techniques. The results reveal spectral detail of an interesting transition region between the nozzle turbulent boundary layer and the jet shear layer in which flow time scales are exceptionally small and spectral signatures of large scale instabilities are superimposed on the incoming boundary layer turbulence. The results point toward the importance of very high frequency coherent phenomena in this region, particularly evident in the radial and shear stresses time-delay behavior.

2.2 Introduction

In recent years, jet noise has become a growing concern worldwide. The sound pollution near large airports and military bases created by jet aircraft taking off and landing has had a large effect on the quality of living in the surrounding areas. Crews onboard the decks of aircraft carriers undergo extreme strain on their inner ears due to the tactical aircraft take-offs and landings that are constantly underway. The consequences of the noise include: costs to treat veterans with hearing damage and the depreciation of property values around airports, both of which may be mitigated by reducing the severity of tactical engine exhaust noise; a task requiring in-depth understanding of the noise source mechanisms in these complex flows.

Several studies have been conducted in the past in supersonic jets, but few detailed studies with full turbulence statistics have been done in heated jets, particularly at the over-expanded conditions of interest for low altitude flight. As a jet is heated, its velocity increases along with the convective Mach number (Eq. 2.1) of large scale eddies in the shear layer, estimated as[1]

$$M_c = (U_j - U_a)/\bar{a} \tag{2.1}$$

where U_a is the co-flow velocity and $\bar{a}$ the average sound speed of the jet and co-flow streams. As aeroacoustic source efficiency changes considerably with M_c (e.g., Ref. 2), the increased convective Mach number of hot jets plays a major role in turbulent noise generation of exhaust flows. The combination of convective amplification and the role that Reynolds stresses play as a key source term in acoustic analogies[3], makes the intense noise due to the non-equilibrium shear layer near hot jet nozzle exits an important topic for earnest consideration.

Facilities like Lockheed Martin's supersonic hot jet noise facility in Marietta, Georgia[4] and the acoustic jet chamber at the National Center for Physical Acoustics at the University of Mississippi[5] use propane burners to generate a heated flow with static temperatures in excess of 1200°F. NASA Glen's Small Hot Jet Acoustic Rig[6] (SHJAR) uses a hydrogen combustor to achieve a total temperature ratio (TTR) of up to 2.8. The main drawback of a combustion based facility is that it vitiates the flow, and creates variable gas mixture with a new specific gas constant. Others choose to use electric heaters, such as the researchers at Florida State University[7], avoiding the issue of vitiation. An alternative approach to simulating hot jet noise is presented by Doty and McLaughlin of The Pennsylvania State University[8], by using helium mixed with compressed air to increase the sound speed of the jet fluid to match heated sound speed conditions. Unfortunately, such a facility cannot match both the jet density and acoustic velocity of a heated flow at the same time, leading to uncertainties in proper simulation of the turbulence structure of high-speed jets. For these reasons, the present authors have decided to create an electrically heated jet facility.

Microphone measurements can be paired with velocity measurements to shed light on the fluid mechanisms in certain acoustic signatures (e.g. Ref. 9). The stochastic, distributed nature of noise-generating compressible turbulence requires a spatio-temporally resolved statistical characterization of its behavior. Several techniques, limited by available technologies, have been brought to bear in the study of supersonic jet characteristics. In several past studies, shadowgraph or Schlieren photography has been used to qualitatively investigate eddy motion[10]. Murakami and Papamouschou[11] have used planar laser-induced fluorescence for visualization of eddy convection. Much of the existing data in supersonic jets was obtained using hot-wire anemometry[10]. While providing valuable information, hot-wires suffer from the formation of wakes and shocks, limited frequency response and difficulty of application in hot flows. Particle Image Velocimetry (PIV) has been used extensively in hot supersonic jet flows by Bridges and Wernet[6,12] but recent examinations of the technique for determining the convection velocity

based on power spectra in low speed turbulent flows revealed that the concept is severely hampered by the restrictions caused by the low-pass filtering behavior of PIV[13]. Despite PIV's drawbacks, Bridges and Wernet were able to acquire streamwise velocity spectra using an advanced time-resolved system, providing extensive information over a wide range of streamwise locations in the developing shear layers of supersonic jets[12]. Lau, Morris, and Fisher[14] show the worth of LDV for measuring Reynolds stresses in the development region of ideally expanded supersonic jets, providing a similarity correlation for the shear layer development which has stood the test of time. Lau[15] and Kehrevé et al.[16] have applied 2-point LDV to cold supersonic jets, exhibiting the potential for the technique in providing convective information.

2.3 Hot Supersonic Jet Facility

A photograph of the supersonic hot jet facility at Virginia Tech is provided in Fig. 2.1. Compressed air for the jet is provided by an Ingersoll-Rand Type 4-HHE-4 4-stage reciprocating air compressor which pressurizes two reservoir tanks with a total volume of 23 m^3 (6,000 gallons) up to 2.0 MPa (300psig). This allows the facility to be continuously run for a range of Mach numbers between 1 and 2. The high pressure air is passed through a dryer to remove moisture before the air enters the jet facility. The facility employs a Sylvania 192 kW Flanged Inline Heater (Model 073153) which has a nominal pipe size of 203 mm (8") and an overall length of 584 mm (23"). This heater supplies the facility with a total temperature at the exit up to 922 K (1200°F) at 0.25 kg/s mass flow rate. The sections downstream of the heater are devoted to flow conditioning (Fig. 2) based

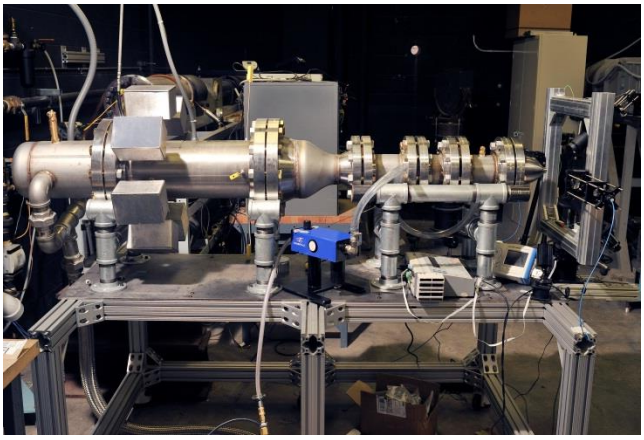

Figure 2.1. Photo of Virginia Tech's supersonic hot jet facility.

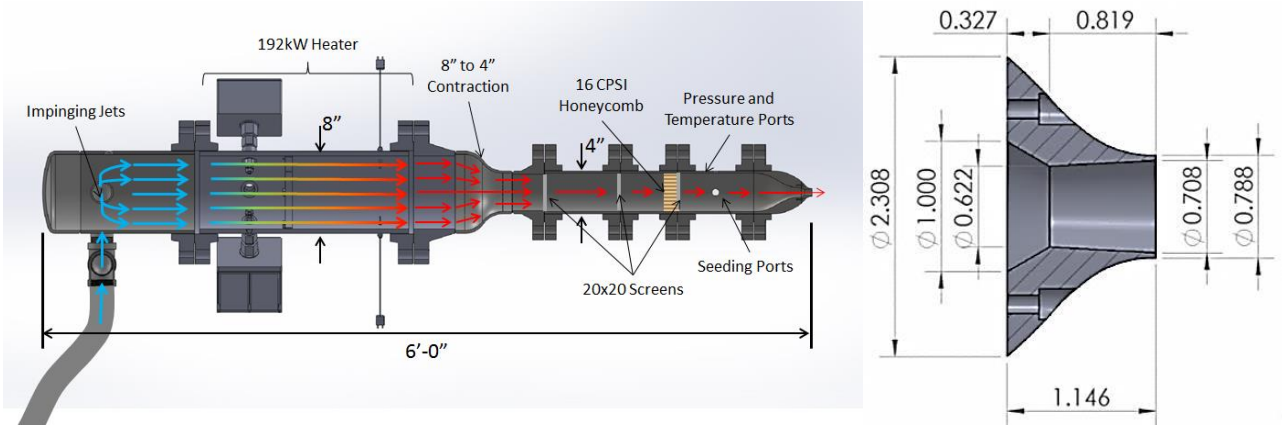

Figure 2.2. (Left) Overview diagram of the new supersonic hot jet facility, detailing the flow conditioning used. (Right) Cross-section diagram of the Mach 1.65 bi-conic nozzle used for the current study (dimensions in inches).

on principles presented by Mehta and Bradshaw[17]. It features three 20 mesh stainless steel screens sandwiched between high temperature gaskets and a 50.8 mm (2") thick piece of honeycomb with a cell length/width ratio of 8. The converging/diverging nozzles at the exit are quickly interchangeable. For the current study, measurements are made with two similar bi-conic nozzles with design Mach number of 1.65 and nozzle pressure ratio (NPR) of 4.58. Fig. 2.2 illustrates the dimensions of the nozzle examined in cold flow results presented, having an exit diameter of 18 mm (0.708") and an exit-to-throat area ratio of 1.295. The hot jet experiments were run with a 38.1 mm (1.5") exit diameter nozzle. At cold conditions an oil-based liquid and pneumatic aerosol generator was used to seed the flow, while at heated conditions 0.3 μm alumina particles were dispersed into the plenum using a fluidized bed seeder. In both instances, a seeding injection bar was used to introduce seed into the jet flow at the location indicated in Fig. 2.2 (left). Note that an additional development length after seed introduction of approximately 610 mm (24") compared with that depicted in Fig. 2.2 is allowed in the nozzle tested for the hot jet measurements.

2.4 Measurement Techniques

Laser Doppler velocimetry has been paired with high-speed shadowgraph videos and far-field microphone measurements for phenomenological interpretations of results. It is crucial that all the measurements be well resolved in both time and space in order to capture the scales of motion which combine to contribute to the jet noise field. Though not presented herein, the facility also has Doppler Global Velocimetry instrumentation for three-component point-wise velocimetry that is currently being expanded for time resolved planar measurements of the Reynolds stress tensor[18].

2.4.1 High-Speed Shadowgraph

A Photron Fastcam SA4 high-speed camera is used to acquire high-speed shadowgraph videos of the hot supersonic jets. A combined reflective/refractive shadowgraph/Schlieren system is used in the measurements, and a continuous illumination xenon light source provides very high illumination levels for very short exposure times. In work presented herein, movies at a nozzle pressure ratio (NPR) of 3.2 centered on the first three shock cells have been acquired in the cold jet at 86,400 frames per second and 3.36 μs single frame expose times. Higher frame rates can be achieved, but a smaller frame would have to be imposed.

2.4.2 Microphone Measurements

Jet noise can be divided into three main components: turbulent mixing noise, broadband shock-associated noise, and screech tones. A dominant source in the cold jet studies presented herein is screech. In order to exhibit the capabilities of the present measurement technique, the attributes of the unsteady flow field leading to screech are considered further. The screech tone

primarily radiates in the upstream direction, while the first harmonic primarily radiates perpendicular to the jet flow direction[19]. Microphone measurements at 90° and 100 diameters from the nozzle reveal the strong presence of the first harmonic of the screech tone for over-expanded NPR ranges. A B&K 4191 microphone was employed for these measurements. The frequency spectra acquired can be seen in Fig. 2.3 for multiple nozzle pressure ratios. These measurements were acquired in a non-anechoic arrangement and were intended only to quantify frequencies of screech tones for verification of the flow kinematics data.

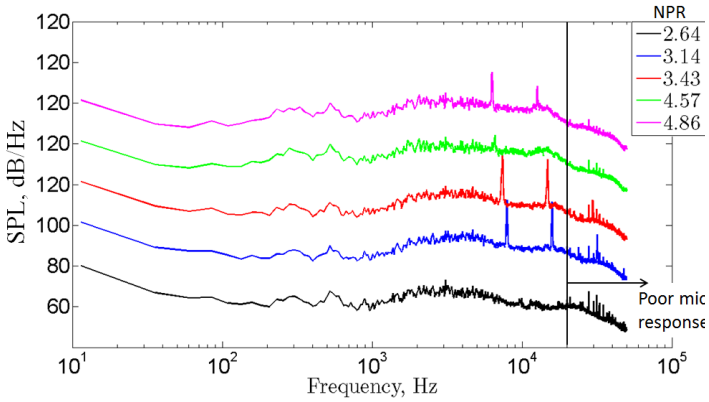

Figure 2.3. Plot of 90^o microphone acoustic spectra at multiple nozzle pressure ratios.

2.4.3 Laser Doppler Velocimetry

As a preliminary investigation into the flow physics of a screeching over-expanded jet, an advanced two component, spatially resolved, single transceiving lens, laser Doppler velocimeter (LDV) was used to acquire velocity measurements within the jet core. The new LDV has a measurement volume diameter of 60 μm and a fringe spacing of approximately 2.03 μm. This probe has a random single-sample uncertainty of $\delta u/U = 0.33\%$. Photos of the two-component LDV used in this study can be seen in Fig. 2.4. For the cold jet measurements, data acquisition and burst processing were controlled using the AUR Studio software suite developed by AUR Inc. Additional details on the burst processing algorithm are discussed by Lowe and Simpson[20].

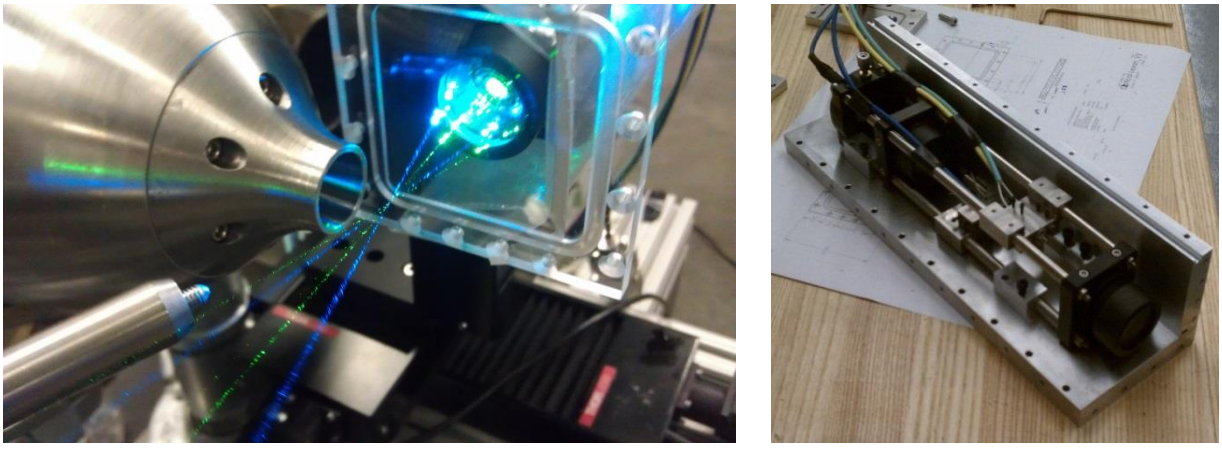

Figure 2.4. (Left) Photo of the two-component LDV mounted at the exit of the supersonic hot jet facility. (Right) Photo of the two-component LDV with part of its case removed.

The acquired LDV velocity measurements are highly resolved, both spatially and temporally. The high sampling rates allow for the calculation of velocity spectra. The LDV data are only acquired when a particle is within the measurement volume, leading to an unevenly sampled data set. The data must be resampled to regular time intervals before any further analysis can be done. It has been shown by Benedict et al.[21] that the best resampling method is known as the fuzzy-slotting method, presented by Müller et al.[22] as an improvement of the slotting method originally created by Mayo et al.[23]. This method allows for the original time series of velocity to be divided into bins constructed according to arrival time-delay. With the fuzzy-slotting scheme, each sample within the bin has a probability weighting assigned to it based on its proximity to the center of the defined bin. The fuzzy-slotting time-delay correlation coefficient is computed as

$$\hat{R}_{uv}(n\Delta\tau) = \frac{\sum_{i=1}^{N}\sum_{j=1}^{N} u_i v_j b_n(t_i - t_j)}{\sum_{i=1}^{N}\sum_{j=1}^{N} b_n(t_i - t_j)} \sum_{i=1}^{N}\sum_{j=1}^{N} u_i v_j b_n(t_i - t_j) \qquad (2.2)$$

$$where \quad b_n(t_i - t_j) = \begin{cases} 1 - \left|\frac{t_i - t_j}{\Delta\tau} - n\right| & for \ \left|\frac{t_i - t_j}{\Delta\tau} - n\right| < 1 \\ 0 & otherwise \end{cases}$$

All time-delay and spectral data presented in this paper were obtained by application of Eq. 2.2 to the randomly sampled LDV data.

2.5 Cold Jet Centerline Results

As a preliminary validation of the spectra measurement concept, the Mach 1.65 bi-conic nozzle case was run at TTR=1, NPR=3.2, creating a screeching, over-expanded condition with a Strouhal number of 1 at 25.3 kHz. The jet conditions can be seen in Table 2.1. A centerline velocity profile was taken from the exit of the nozzle out to four diameters downstream. This measurement region covers the first three shock cells (and part of the fourth) and is fully within the potential core. The first shock cell remains stable over time, while the following cells are unstable, as observed in high-speed shadowgraph videos. The LDV probe allowed measurement of two components of velocity (streamwise and radial). The streamwise mean velocities are

Table 2.1. Cold jet conditions

M_j	1.65	P_0	307 kPa
U_j	456 m/s	P_a	96 kPa
Re_d	1.1 M	T_0	294 K
T_j	190 K	T_a	294 K

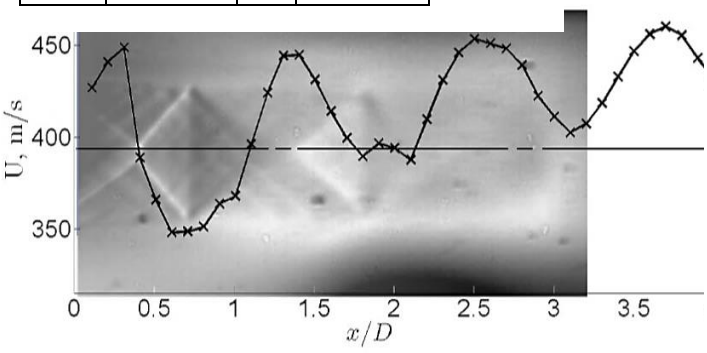

Figure 2.5. Plot of the mean streamwise velocity from the nozzle exit to four diameters downstream, superimposed on a shadowgraph image.

presented in Fig. 2.5, overlaid upon a shadowgraph image of the shock structure. The increase in peak jet velocity for this case is most likely due to the non-uniform exit velocity characteristic of bi-conic nozzles in combination with the violent core motions due to screech.

Using the fuzzy-slotting method, the time-delay autocorrelation of the resampled streamwise velocity measurements can be seen in Fig. 2.6. Contour plots of Reynolds stress power spectral density as a function of frequency and distance from the exit plane of the nozzle are shown in Fig. 2.7. These plots show that the fundamental screech tone (verified using the microphone data of Fig. 2.3) shows up in the Reynolds stresses after 0.5 diameters, and the first harmonic shows up after 2 diameters. In the streamwise component of velocity, the second and third harmonic can even be seen. The low frequency energy in the streamwise spectra near the nozzle exit can be attributed to variations introduced by the controller used to set the NPR of the facility, as the fluctuations are not present in the radial normal stress spectra.

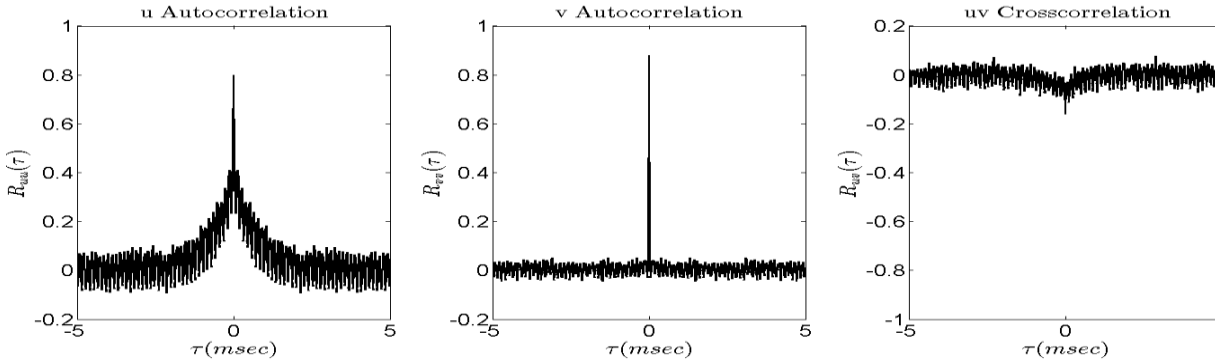

Figure 2.6. Plots of the autocorrelation functions for the streamwise and vertical components of velocity, as well as the cross-correlation of the two components at a station located at one diameter downstream of the nozzle exit.

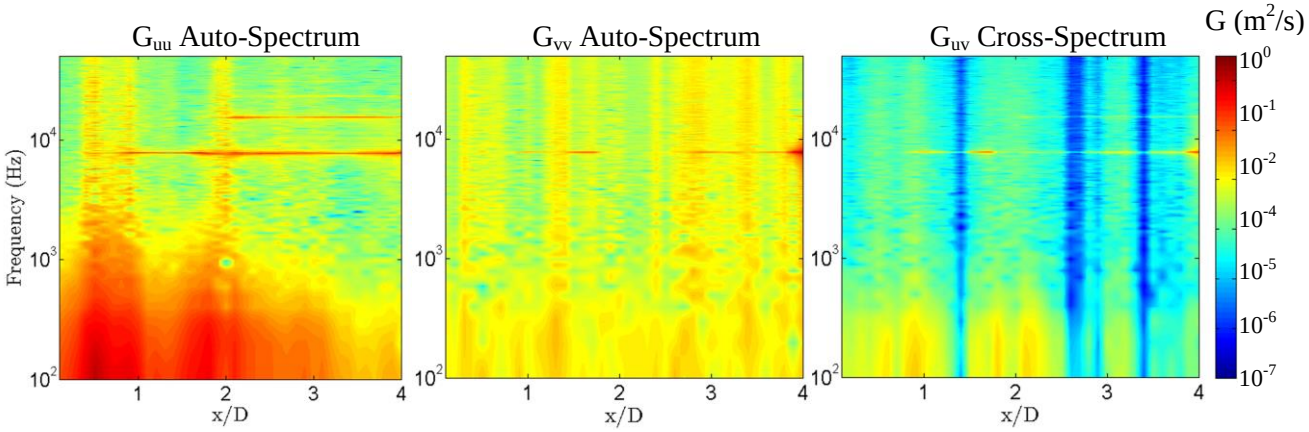

Figure 2.7. Plot of the frequency domain for streamwise stations ranging from the nozzle ex to four diameters downstream. (Left) Streamwise Reynolds Stress (Center) Vertical Reynolds Stress (Right) Reynolds Shear Stress

It can be seen that the acoustic screech tone measured by the microphone at 90° directivity shows up in the frequency domain of the measured Reynolds stress spectra at approximately 7,800 Hz. The first harmonic begins to develop downstream of the first two shock cells at approximately 15,300 Hz. This location corresponds to where the shock structure appears to become unstable in shadowgraph videos. Fig. 2.8 shows the development of the power spectral density of the streamwise Reynolds normal stress at the screech tone frequency and its first harmonic over the first four diameters of the jet core. It can be seen that from 0 to 0.75 diameters neither tone is prominent. From 0.75 to 2 diameters, the fundamental screech tone is dominant and from 2 to 3.75 diameters, both tones are seen well above the narrowband spectral levels around the primary and harmonic frequencies in the stress spectra. At 4 diameters downstream it appears as though the same mode of fundamental tone dominance as 0.75 to 2 diameters reappears. Although, pending further data, this assertion is speculative.

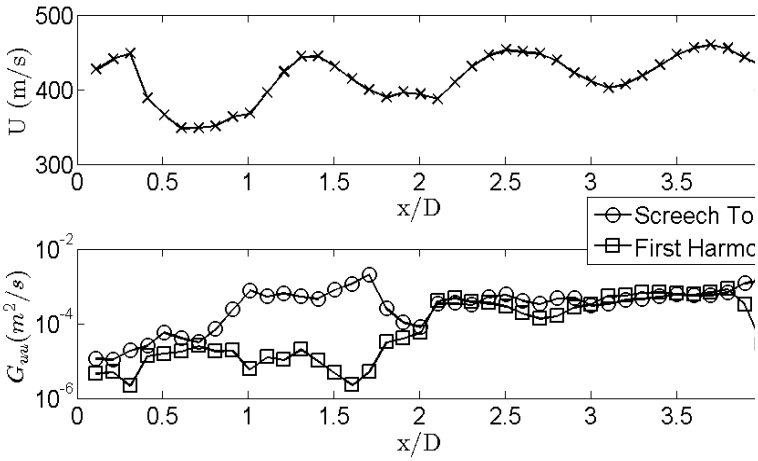

Figure 2.8. Plot of mean spanwise velocity compared to a plot of the amplitude of the screech tone and its first harmonic.

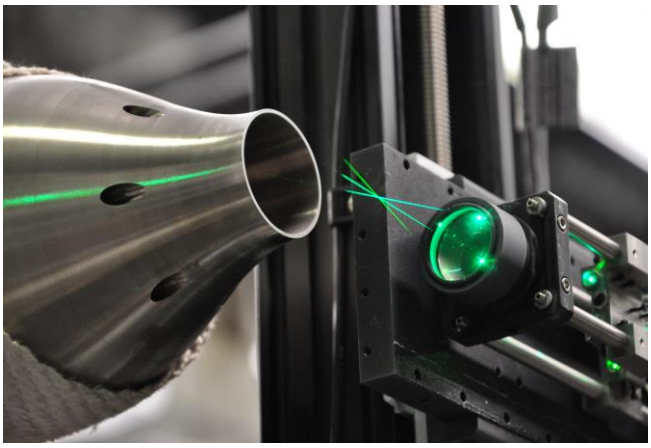

Figure 2.9. Photo of the two-component LDV measuring at the lower lip line of the supersonic hot jet facility with the 1.5" exit diameter nozzle.

2.6 Heated Jet Shear Layer Results

Initial results are presented of a measurement campaign to map the Reynolds stress spectra in the shear layer of a Mach 1.65 bi-conic nozzle with an exit diameter of 38.1mm (1.5"). In the data presented below, the nozzle is run at the design pressure condition (NPR = 4.58) and heated to TTR = 2. The jet conditions are presented in Table 2.2.

Table 2.2. Heated jet conditions

M_j	1.65	P_0	441 kPa
U_j	642 m/s	P_a	96 kPa
Re_d	1.1 M	T_0	577 K

The procedure for data acquisition of heated cases include:

1. Heating the facility to the desired TTR at an NPR of 4.58 until steady-state conditions were observed in the stainless steel facility vessel
2. Traversing the LDV probe volume to the lower nozzle lip to optically find the position of the nozzle lip after thermal expansion.
3. Setting a datum at the location where the first Doppler burst signals could be observed within the core stream directly at the exit
4. Traversing the LDV probe downstream to the first measurement location (Fig. 2.9)

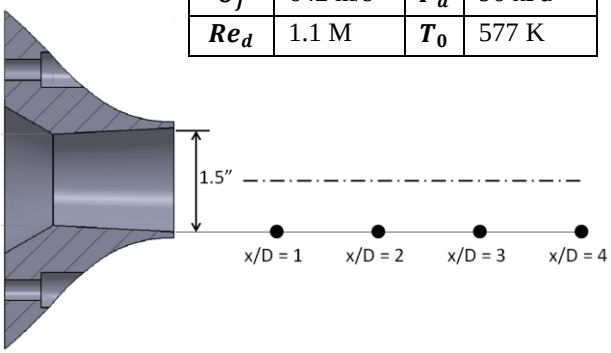

Figure 2.10. Diagram of measuring locations on the lip line.

As an initial study, four points (x/D = 1,2,3,4) were acquired along the lip line (r/D = 0.5) of the nozzle (Fig. 2.10) using the two-component LDV. The LDV beam/nozzle configuration for the 1.5" diameter nozzle is shown in Fig. 2.9. At each point, 100 files containing 16*m*s of raw photomultiplier signal data each were acquired. These signals were stored in their entirety to a local solid state hard drive for offline burst processing. As in the cold jet study, a PSD-based single-burst post-processor was used. At these near-nozzle points, the burst processor returned velocities of approximately 30% of the jet core velocity. The resulting velocity samples obtained were run through the slot correlation method (Eq. 2.2). Even in this limited dataset, several interesting preliminary results are obtained in the Reynolds stress time-delay correlations and power spectra.

The time-delay correlation coefficient for the four streamwise stations can be seen in Fig. 2.11. As one would expect due to the rapidly growing shear layer in the near-nozzle region, the streamwise component exhibits a widening of the correlation function with an increase in streamwise position. The axial integral time-scale was computed for each of these points, their evolution plotted in Fig. 2.12. A linear fit to the data yields the following correlation:

$$T = (3.1259\, x/D + 6.1294) \tag{2.3}$$

thus revealing the dominance of very small time-scales, even at these radial locations of only 30% the jet bulk exit velocity.

The radial Reynolds stress correlation (v autocorrelation) indicates the presence of short lived cyclical structures out to a time-delay of approximately 0.025 milliseconds. These features tend to increase in time-scale and decrease in amplitude relative to the peak correlation coefficient as one progresses downstream. Although further evidence is needed, the signatures

are consistent with the formation and growth of low order wave packets which are transitioning into multi-scale turbulent eddies. The cross-correlation coefficient (*uv*) similarly to streamwise and radial stresses, exhibits rapidly growing time-scales. The shape of the correlation is consistent with those obtained in past studies, exhibiting a negative time delay behavior which rapidly decreases to a minimum at a time-delay just greater than zero. The subsequent relaxation for positive delay follows with a much greater time-scale. This behavior is commonly observed shear flow coherent structure events, wherein the head of an eddy will abruptly eject high momentum fluid toward the outer radii region while the tail of the same eddy pulls low momentum flow toward the core over a greater region.

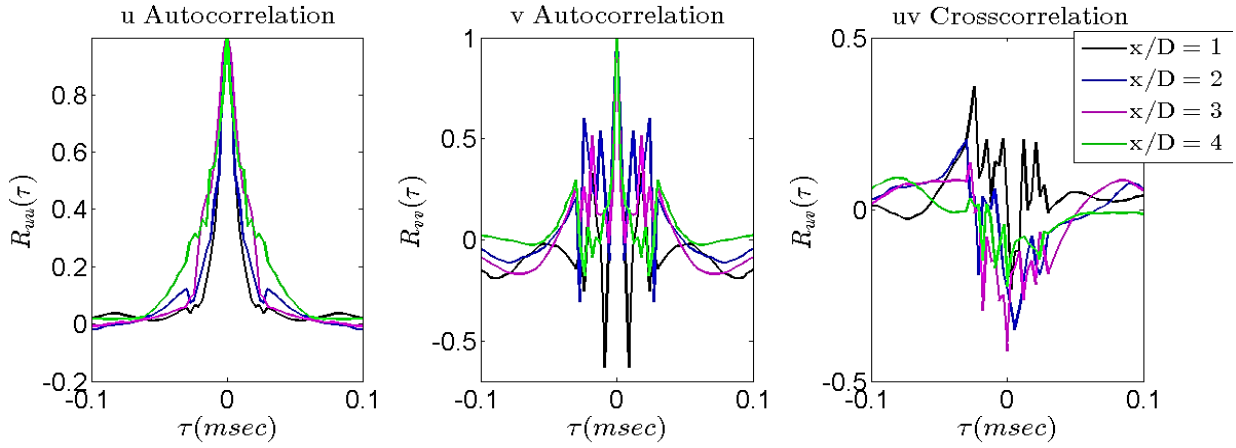

Figure 2.11. Rescaled plots of the autocorrelation functions for the streamwise and radial components of velocity, as well as the cross-correlation of the two components at *x/D* = 1,2,3,4.

The Reynolds stress power spectral densities computed from the time-delay correlations for u^2 is shown in Fig. 2.13. The spectra for the streamwise velocity component exhibit an overlap region with a -5/3 slope, particularly for the point nearest the nozzle exit. While further results are being analyzed to confirm this assessment, it is most likely the case that the nozzle internal boundary layer at the exit is turbulent based upon the spectral behavior. This could be due to the large Reynolds number of the flow or due to the sharp point at the throat of the bi-conic nozzle. Of particular note in the streamwise spectra is the transition between the turbulent spectrum, near the exit, to the spectra exhibiting evidence of strong shear layer instability modes at both high and low frequencies. The flow appears to evolve as a superposition of turbulent eddies carried along with shear layer instability features.

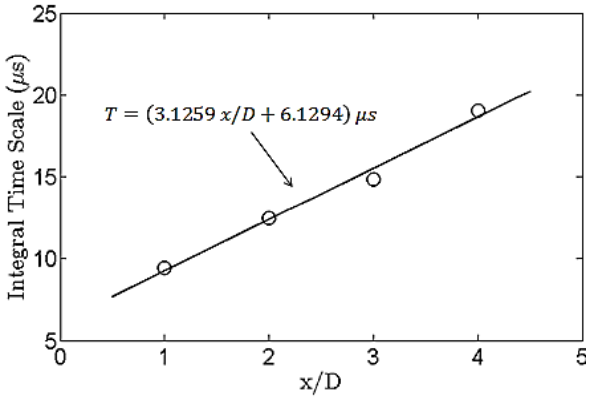

Figure 2.12. Plot of the integral time scales as a function of streamwise location.

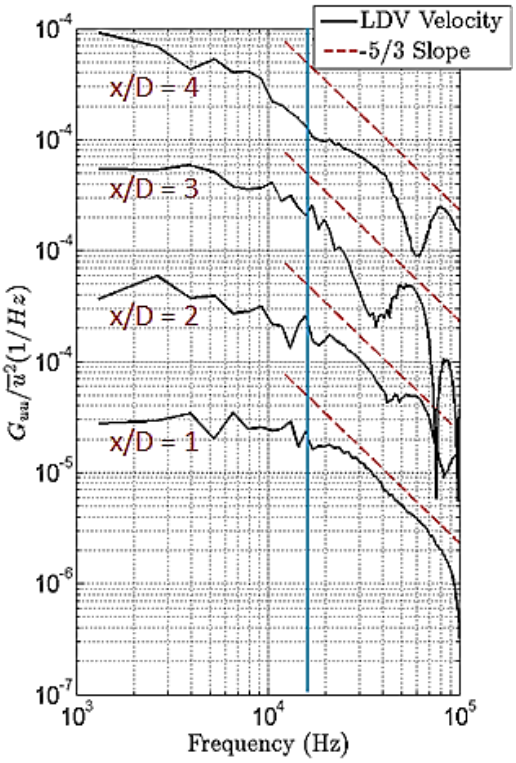

Figure 2.13. Streamwise Reynolds stress spectra for streamwise stations *x/D* = 1,2,3,4 (each station is separated by a vertical decade, *x/D* = 1 is at the bottom and *x/D* = 4 is at the top). The blue line denotes a Strouhal number of 1 (16.8 kHz).

The streamwise Reynolds stress spectra from the current study were compared to the previous works of Kerhervé et al.[16] and Kuo et al.[24] Fig. 2.14 shows the streamwise Reynolds stress at *x/D* = 2 and 3 compared to Kerhervé's spectra at the same locations in a cold Mach 1.2 jet using an LDV. The spectral shapes at both locations show good agreement with the current study, although some differences exist in the distribution of low and high frequency energy (e.g., the current study appears to reveal a greater contribution from higher frequencies than was observed in the cold jet). Fig. 2.14 also shows

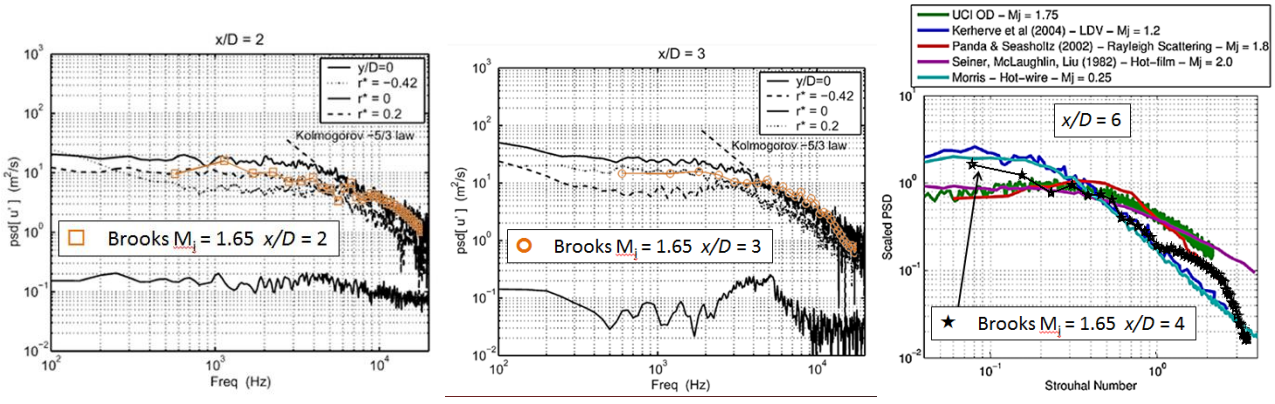

Figure 2.14. Comparison of the streamwise Reynolds stress results with past studies [16, 24]. (Left) *x/D* = 2 [16] (Center) *x/D* = 3 [16] (Right) *x/D* = 4 compared with previous data at *x/D* = 6 [24,25].

the current streamwise Reynolds stress spectra at $x/D = 4$ as compared to a compilation of data presented by Kuo et al., which also contains the Kerhervé's data, all at an $x/D = 6$. The currently presented LDV data matches well with the Kerhervé's LDV data and the hot-wire data from Morris[25]. Further investigation is required to determine why there is a difference in the high frequency behavior of the spectrum above a Strouhal number of 1. Finally, it is possible to note that all compiled sets of velocimetry results indicate a fundamentally different spectral behavior from the compiled data based upon density techniques (Rayleigh scattering and optical deflectometry). These findings motivate further examination of the spectral behavior and evolution.

2.7 Future Work

In the near future, the authors will extend the work done in the supersonic jet rig at Virginia Tech to include more measurement points at heated conditions, both in the streamwise (out to $x/D = 8$) and radial directions. This will better show relationships and trends in the evolution of the turbulence, instabilities, and turbulence/instability interactions in the jet flow. Also, two-point LDV measurements will be made to investigate space-time correlations and convective wave speed. The authors will then use these new insights into the turbulence to directly impact the understanding of the acoustic field generated by such a flow.

2.8 Conclusions

Measurements of velocity and Reynolds stress have been acquired with a two-component laser Doppler velocimeter at high data rates in Virginia Tech's new heated supersonic jet facility. Two specific measurement campaigns were presented: an investigation into the development of centerline Reynolds stress spectra of an over-expanded jet at cold conditions and an investigation into the near-nozzle shear layer development at design nozzle pressure ratio and a total temperature ratio of 2. The cold tests gave the researchers the confidence needed in the new facility and instrument to pursue heated tests. To note from the cold study, the local appearance of the screech tone and harmonics along the centerline of the jet within the first four diameters is assessed in Reynolds stress spectra, indicating that harmonics are introduced progressively with shock cell number. In the heated study, the region investigated shows transition between the nozzle turbulent boundary layer and the jet shear layer. In this region the flow time scales are exceptionally small and the spectral signatures of large scale instabilities are superimposed on the incoming boundary layer turbulence. It was also shown that high frequency turbulence phenomena are important in the radial and shear stresses in the region of the near nozzle region of the flow. The Reynolds stress spectra that were obtained in this study show similarity to data obtained in past studies, with better agreement seen between velocimetry techniques than techniques based upon density. Generally, the current study revealed spectral shapes with greater high frequency content that was exhibited in previous studies of cold jets.

2.9 Acknowledgements

The authors would like to acknowledge the support of the Office of Naval Research through the Hot Jet Noise Reduction Basic Research Challenge, Drs. Brenda Henderson and Joseph Doychak, program managers (Grants N00014-11-1-0754 and N00014-12-1-0803). The work was also supported by the Virginia Tech Department of Aerospace and Ocean Engineering. The presentation of results benefited from several discussions with Profs. Dennis McLaughlin and Philip Morris of the Department of Aerospace Engineering at The Pennsylvania State University. We would also like to acknowledge the machinists of the Department of Aerospace and Ocean Engineering for the precision parts used in the probe and Applied University Research and Dr. Roger Simpson for the support of AUR Studio, the LDV acquisition software used.

2.10 References

[1]Lin, C.C., "On the Stability of the Laminar Mixing Region Between Two Parallel Streams in a Gas," *NACA-TN*, No. 2887, 1953.

[2]Crighton, D.G., "Basic Principles of Aerodynamic Noise Generation," *Prog. Aerospace Sci.*, Vol. 16, No. 1, 1975, pp. 31-96.

[3]Lighthill, M., "On sound generated aerodynamically. I. General theory," Proceedings of the Royal Society of London, 1952, pp. 1-25.

[4]Tanna, H.K., Fisher, M.J., Dean, P.D., "Effect of Temperature on Supersonic Jet Noise," *AIAA Aero-Acoustics*, No. 991, 1973.

[5]Baars, W.J., Tinney, C.E., Murray, N.E., Jansen, B.J., and Panickar, P., "The Effect of Heat on Turbulent Mixing Noise in Supersonic Jets," *AIAA Aerospace Science Meeting*, Vol. 49, No. 2011-1029, 2011, pp. 44-46.

[6]Bridges, J., and Wernet, M.P., "Turbulence Associated with Broadband Shock Noise in Hot Jets," *29th AIAA Aeroacoustics Confrence*, No. 2834, 2008.

[7]Wishart, D.P., Krothapalli, A., "On the Structure of a Heated Supersonic Jet," *AIAA 32nd Aerospace Science Meeting*, No. 0666, 1994.

[8]Doty, M. J., and McLaughlin, D. K., "Acoustic and Mean Flow Measurements of High-Speed, Helium/Air Mixture Jets," *International Journal of Aeroacoustics*, Vol. 2, No. 3, 2003, pp. 293–334.

[9]Papamoschou, D., Morris, P.J., and McLaughlin, D.K., "Beamformed Flow-Acoustic Correlations in High-Speed Jets," *AIAA Paper*, No. 3212, 2009.

[10]Papamoschou, D., Roshko, A., "The Compressible Turbulent Shear layer: An Experimental Study," *J. Fluid Mech.*, Vol. 197, 1988, pp. 453-477.

[11]Murakami, E., Papamoschou, D., "Eddy Convection in Coaxial Supersonic Jets," *AIAA Journal*, Vol. 38, No. 4, 2000, pp.628-635.

[12]Bridges, J., Wernet, M., "Measurements of the Aeroacoustic Sound Source in Hot Jets," 2003 AIAA–2003–3130

[13]De Kat, R., Gan, L., Dawson, J., Ganapathisubramani, B. "Limitations of Estimating Turbulent Convection Velocities from PIV," *Int. Symp. On Application of Laser Techniques to Fluid Mechanics*, Vol. 16, 2012.

[14]Lau, J.C., Morris, P.J., and Fisher, M.J., "Measurements in subsonic and supersonic free jets using a laser velocimeter," *Journal of Fluid Mechanics*, Vol. 93, No. 1, 1979, pp. 1-27.

[15]Lau, J.C., "Laser Velocimeter Correlation Measurements in Subsonic and Supersonic Jets," *Journal of Sound and Vibration*, Vol. 70, 1980, pp. 85-101.

[16]Kerhervé, F., Jordan, P., Gervais, Y., Valière J.C., Braud, P., "Two-Point Laser Doppler Velocimetry Measurements in a Mach 1.2 Cold Supersonic Jet for Statistical Aeroacoustic Source Model," *Exp. In Fluids*, Vol. 37, 2004, pp. 419-437

[17]Mehta, R., Bradshaw, P., "Design Rules for Small Low Speed Wind Tunnels," *Aeronautical Journal of the Royal Aeronautical Society*, 1979, pp. 442-449.

[18] Ecker, T., Brooks, D. R., Lowe, K. T., Ng, W., "Spectral analysis of over-expanded cold jets via 3-component point Doppler velocimetry," *AIAA Scitech (52nd Aerospace Sciences Meeting)*, 2014.

[19]Tam, C., "Supersonic Jet Noise," *Annu. Rev. Fluid Mech.*, Vol. 27, 1995, pp. 17-43.

[20]Lowe, K.T., and Simpson, R.L., "A Laser-Doppler Velocimeter System for Near-Field Velocity Vector Measurements in Large Facilities," *AIAA 50th Aerospace Science Meeting*, No. 0693, 2012.

[21]Benedict, L.H., Nobach, H., and Tropea, C., "Estimation of turbulent velocity spectra from laser-Doppler data," *Meas. Sci. Tech.* Vol. 11, 2011, pp. 1089-1104.

[22]Müller, E., Nobach, H., and Tropea C., "Model parameter estimation from nonequidistant sampled data sets at low data rates," *Meas. Sci. Technol.*, Vol. 9, 1998, pp. 435–41.

[23]Mayo, W.T. Jr., Shay, M.T., and Ritter, S., "Digital estimation of turbulence power spectra from burst counter LDV data," *Proc. 2nd Int. Workshop on Laser Velocimetry*, Purdue Univerisity, 1974, pp. 16-26.

[24]Kuo, C., Powers, R., McLaughlin, D., "Space-time correlation of flow and acoustic field measurements in supersonic helium-air mixture jets using optical deflectometry," *32nd AIAA Aeroacoustics Conf.*, 2011, pp. 1-24.

[25]Morris, P.J., Zaman, K.B., "Velocity measurements in jets with application to noise source modeling," *Journal of Sound and Vibration*. 2010, pp. 394-414.